Jurnal Tribologi 40 (2024) 212-225

Jurnal Tribologi
Website : jurnaltribologi.mytribos.org e-issn: 2289-7232

Experimental investigation on the physical, mechanical, and tribological behavior of brake friction composites for railway application

Sindhu Budati, Mohd Hafis Sulaiman *, Zulkifli Leman, Mohd Zuhri Mohamed Yusoff, Edi Syams Zainudin

Department of Mechanical and Manufacturing Engineering, Faculty of Engineering, Universiti Putra Malaysia, 43400 Serdang, Selangor, MALAYSIA.
*Corresponding author: hafissulaiman@upm.edu.my

KEYWORDS

Composite
Brake material
Hemp
Rice husk
Phenolic resin

ABSTRACT

Non asbestos brake friction composites with hemp fibre and rice husk (RH) reinforcements (20 weight %) were developed and characterized for physical, mechanical and tribological properties. The properties such as density, porosity, hardness (ASTM D785-03 standard HRR scale), impact strength, and wear rate (block-on-ring test ASTM G77 standard) were measured and compared with commercial brake block material sample. The experiment results showed that the hemp fibre-based composite has higher density (1.407 g/cm^3), specific wear rate (0.164×10^{-2} mm^3/Nm) and impact strength values than the RH reinforced composites. RH has higher impact strength (6 KJ/m^2) and hardness (93.06 HRR) than the commercial brake block and hemp composite materials. From the evaluated results it can be concluded that Hemp reinforced phenolic composites can be used as alternative for existing brake materials. Dino lite digital microscope was used to examine the wear mechanism of the worn surfaces.

Received 14 October 2023; received in revised form 17 December 2023; accepted 22 January 2024.
To cite this article: Budati et al., (2024). Experimental investigation on the physical, mechanical, and tribological behavior of brake friction composites for railway application. Jurnal Tribologi 40, pp.212-225.

1.0 INTRODUCTION

A composite is one made of two or more different materials that have diverse chemical, physical, and mechanical qualities. When these components are combined, a new material is created that differs from the constituent materials in terms of its attributes. Matrix and fibre (reinforcement) are the two main types of materials that make up composite materials (Le Bell et al., 2007) Both serve different purposes; the matrix binds the fibre and acts as glue to the fibre serves as the frame material in composites. The strength of the link between the fibres and the matrix (resin) determines how effectively the fibres in composites prevent crack growth. A combination of the two will result in a stiff, strong, but light material (Rashid et al., 2016).

Brake friction composites contains five types of components reinforcement, binder, filler, friction modifier, and abrasive. The purpose of filler is to decrease production costs, increase production efficiency, and serve as functional modifiers for brakes (Ademoh et al., 2015). Friction modifiers are used to reduce the friction and minimise the damage. Without the need for a liquid medium, solid or dry lubricants can minimise friction between surfaces. Compared to conventional oil-based lubricants, they offer greater lubrication at high temperatures because of their layered molecular structure and weak interlayer bonds, as shown in Figure 1. Abrasives improve compound wear resistance and friction efficiency (Singh et al., 2017).

At varying operating conditions like pressure, speeds, temperature, and other environmental conditions, a consistent coefficient of friction and low wear rate is a must for the friction materials (Ikpambese et al., 2016). The ability of hemp fibre as friction material is currently gaining lot of interest in research due to its recoverable, environmentally friendly, affordable, lightweight, and high specific mechanical performance, among other benefits (Palanivel et al.,2019). These fibres fared better than mineral, aramid, and other fibres with respect to mechanical and friction qualities. Although sisal fibre was utilised to make the brake pad, it cannot sustain high temperatures. The excellent heat resilience of the hemp fibre is seen here. In comparison to other fibres, hemp fibre has a high thermal resistance because of its low heat conductivity of 0.060 W/mK (Naidu et al., 2020). The waste product of rice milling is RH. The crust of the planet contains a lot of RHs. They are therefore utilised as fillers and reinforcement. RHs mostly consist of cellulose, pentosan lignin, and silica. As a result, using RH as a fibre can increase the composite's strength while decreasing its strength since RH and polymer resin have a weak interfacial interaction (Bayu et al., 2022). RH has better coefficient of friction 0.58 than other fibres (Anggraeni et al., 2022).

Binders keep every component in the friction brake block application together, which lowers shear rate of the component. The wear and coefficient of friction of the brake pads are affected by the binder. By tightly fusing the other three components, the binder provides mechanical unity to the components in friction materials, enhancing the characteristics of the composites. Due to their favourable thermal and mechanical characteristics, as well as their cheaper cost, phenolic resins (either synthesized or un-synthesized) have been used as binders in the fabrication of brake materials over the past 50 years (Jeganmohan et al., 2020). For the mixture to be protected from precipitation that could change the heterogeneity of the fibre and the matrix and lead to conglomerate after hardening, the matrix must have a good viscosity (Basim Abdul-Hussein et al., 2015).

Due to their biodegradability, eco-friendliness, and renewability, natural fibres used as a reinforcing element in brake pad composites appear to be a great answer. This makes environmentally friendly materials useful in a variety of applications (Rao & Babji, 2015). Natural fibre-reinforced composites have found a massive diffusion in a variety of technical applications due to their desirable features, such as lightweight, incredible strength, and stiffness (Idris et al., 2015).

In this paper we investigated the effect of hemp fibre and RH on mechanical, physical, and tribological properties of fibre based asbestos free brake pad composites. These results are compared with the behaviour of commercial brake block material.

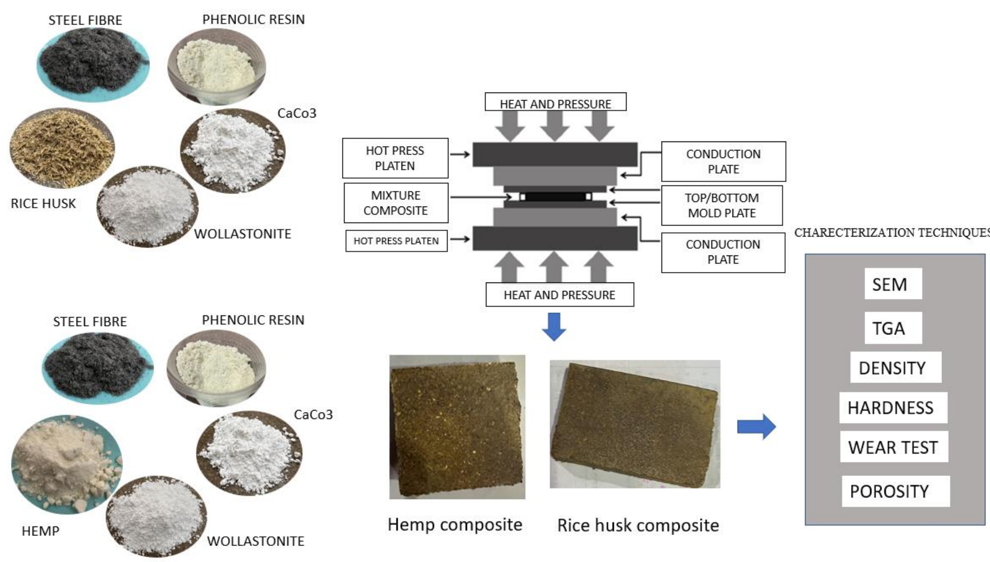

Figure 1: The main material for the composite.

2.0 MATERIALS AND METHODS

2.1 Material Selection

The materials used in this work includes RH, hemp, phenolic resin, steel fibre, wollastonite, and calcium carbonate ($CaCo_3$). The wollastonite (KM25W) was obtained from KAOLIN (MALAYSIA) SDN.BHD, Puchong. The chemical composition shown in Table 1. Steel fibre was obtained from Dezhou Zhenbang Industrial Co. Ltd. The chemical composition of steel fibre showed in Table 2. Calcium carbonate was obtained from KAOLIN (MALAYSIA) SDN.BHD, Puchong. The chemical composition of calcium carbonate is shown in Table 3. Phenolic resin (PF-6801) was obtained from SHANDONG SHENGQUAN NEW MATERIALS CO., LTD, Jinan, China.

RH was obtained from waste of rice mills in the area Puchong, Malaysia. Due to the various geographical situations, types of weather, quality of the soil, and manures employed in the paddy growth, it is discovered that the chemical contents vary. (Article et al., 2020)

RH is robust, water-insoluble, woody, and contains silica-cellulose structure and abrasion resistant behaviour by nature. The inner and middle epidermis have a thin coating of silica, whereas the outer epidermis is largely covered with silica, has a thick cuticle, and includes surface hairs. In Table 4, the components of RH are listed.

The hemp plant is shown in Figure 2. The Hemp leaves were obtained from a plantation in Arau (Perlis, Northern Peninsular Malaysia), and the water retting procedure was used on a lab scale to remove the fibres. Compared to mechanical and chemical procedures, water retting is a cheaper and simpler method. The leaves were first cleaned and chopped. To break down lignin's, hemicelluloses, waxes, and pectin's, the leaves were then submerged in water for 20 days (Shahril et al., 2022). Finally, the individual fibre bundles were separated from the strips, cleaned with running water to get rid of the surface pollutants, and dried outside in the sun for two days.

Figure 2: Mauritius hemp plant.

Table 1: Chemical composition of wollastonite.

Component	Proportion (% w/w)
SiO_2	47.1
CaO	39.9
Al_2O_3	3.9
Fe_2O_3	2.8
TiO_2	0.2
K_2O	0.04
MgO	1.4
Na_2O	0.2
SO_3	0.05
Water	The rest

Table 2: Steel fibre chemical composition.

Component	Proportion (% w/w)
C	0.07 - 0.12 %
Mn	1.25%
Fe	98-99%
P	0.03%
S	0.03%
Si	0.07%
Oil content	0.3%
Fiber width for D1-80 grade	0.036-0.0598
Fiber width for 3-60 grade	0.0889-0.141
P	0.03%

Table 3: Chemical composition and physical properties of calcium carbonate.

Physical Properties		Chemical Properties	
Moisture content	Below 1.0%	Calcium carbonate ($CaCO_3$)	99.5%
PH (30% solid)	7.0-10.0	Calcium (CaO)	53.0 - 58.0%
Brightness	90.0-98.0%	Aluminum (Al_2O_3)	Below 0.1%
325 Mesh residue	Below 3.0%	Silica (SiO_2)	Below 0.1%
Average particle size	10.0 - 15.0 µ	Iron (Fe_2O_3)	Below 0.2%
		Magnesium (MgO)	Below 1.5%
		Loss on Ignition @1025°C	42-46%

Table 4: RH composition.

Constituent	Percentage
Cellulose	35
Hemicelluloses	25
Lignin	20
Crude protein	3
Ash	17

2.2 Material Preparation

The composite samples were prepared by using the hot compression moulding technique. The hemp and RH particles were dried using Memmert model TV 30 U electric oven at 60°C for 22 hours. Two composites with two different compositions as mentioned in Table 5 were fabricated.

All the powders are measured according to weight poured in a container and mixed for 15 minutes. To facilitate easy extraction, the powder mixture was poured into an open steel mould and covered with Teflon sheet. The entire mould setup with composite powder mixture was placed in hot press and compressed at 160 °C for 30 minutes. Then post curing of the fabricated samples was done in an oven at 5 °C for 10 mins. The sample preparation process was shown in Figure 3.

Table 5: Material composition details.

Material	Weight %	Composite 1	Composite 2
Fibre	20	Hemp	RH
Binder	35	Phenolic resin	Phenolic resin
Solid lubricant	5	Wollastonite	Wollastonite
Abrasive	10	Steel fibre	Steel fibre
Filler	30	$CaCo_3$	$CaCo_3$

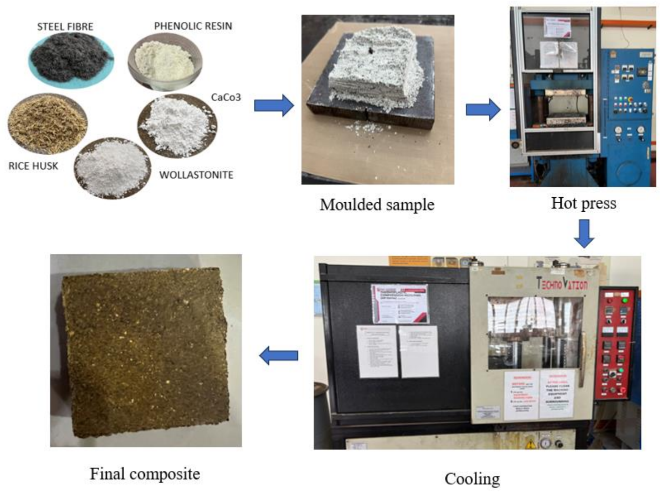

Figure 3: Process of composite preparation.

2.3 Density & Porosity

The composite's density was measured by measuring its mass and volume. Density, mass of a unit volume of a material substance.

Density is $d = m/v$, (1)

Where d is density, m is mass, and v is volume. Density is expressed in units of grams per cubic centimetre. (Patel et al., 2022)

Porosity was measured using fluid displacement method. Porosity is the measure of how many (small) voids there are overall in a substance. An area in a composite which isn't filled with resin or fibre is called a void. Large voids are now seen as independent objects that must be handled at a continuum level rather than as discrete objects with size, form, and precise locations inside the material. Porosity in composite parts can be brought on by a few different things, and achieving zero porosity is extremely difficult. Porosity cannot be totally prevented throughout the casting process, although it can be controlled. The composites' porosity was measured using the equation shown below:

$$\Phi = \frac{V_{dry}}{V_{water}} \tag{2}$$

Where V_{dry} sample is the volume of the dry sample, V_{water} is the volume of water, and Φ is the porosity.

2.4 Hardness

According to ASTM D785-03 standard, with a Rockwell R hardness number (HRR) scale, a 60 N load,10 seconds loading period and a Rockwell hardness tester, a hardness test was performed at room temperature. To achieve the accuracy the surface of the sample was polished.(V et al., 2021) Total 5 samples were measured for hardness and calculated the average hardness value for accurate results.

2.5 Block-On-Ring (Wear Test)

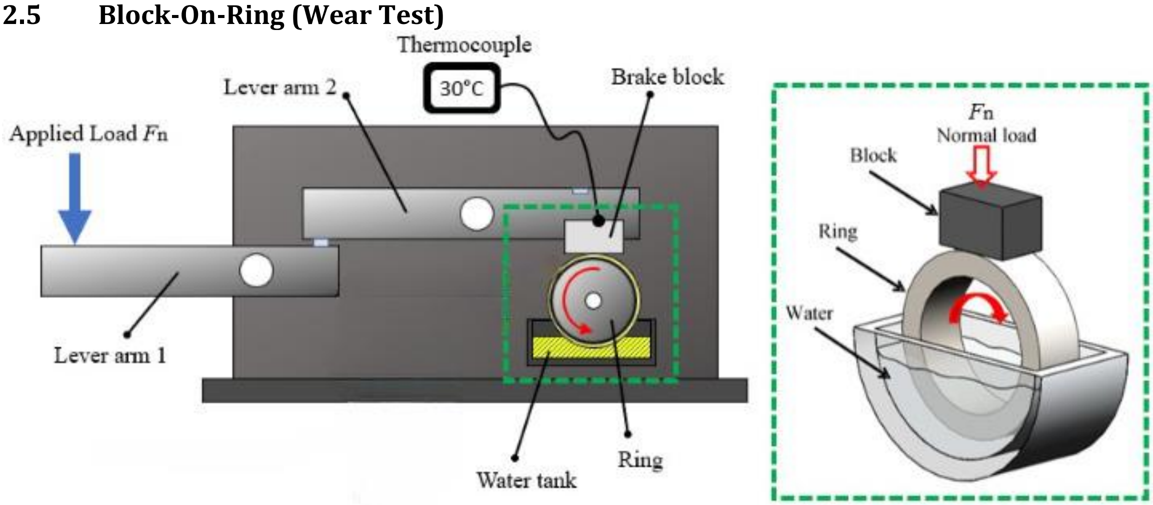

Figure 4 : The Block- on- ring test setup.

The durability test rig was built to simulate actual train braking circumstances. The apparatus was created and designed in compliance with ASTM G77. Brake sample testing has been done with a contact load of 1.2 kg. As shown in Figure 4, the individual 14×14×14 mm^3 brake block is in touch with and parallel to the side of the counter face. The test sample was clamped and pressed against a 22 mm-diameter 58 HRC steel revolving bearing ring. The experimental setup is shown in Figure 4. The ring was polished and cleaned with acetone prior to each test to get rid of any brake dust residue. The brake samples were put through 60-minute durability tests in both dry and rainy circumstances. The block's volume loss after the durability test is recorded. Temperature, friction coefficient, and normal force measurements were measured continuously using ARDUINO IDE software.

Before testing, a counterweight balancer should balance the machine's load lever arm. This is carried out when no load is being applied. Counter faces constructed of different materials, such as cast iron, aluminium, metals, stainless steel, titanium, etc., may differ according on the requirements of the test. This test is frequently used to check for sliding or rolling wear patterns in tyre tread materials, brake pads, pulleys, and camshafts (Budati et al., 2023).

$$Brugger = Test\ load / wear\ area \tag{3}$$

The Brugger value gives better results to differentiate between the performance levels according to wear scar diameter. The Brugger value for RH and hemp samples were measured using equation (3).

2.6 Impact Test

Using INSTRON CEAST 9050, the un-notch Izod impact test was carried out in accordance with ASTM D256. The test sample is struck by a swing pendulum while being supported as a vertical cantilever beam. A rectangular specimen of (3.2×12.7×64) mm^3 was employed for the test, which was performed with a hammer of type 0.5 J. The experimental setup is shown in Figure 5. Five specimens of each fibre load composite were averaged, and the result was calculated. It is possible to analyse the impact energy in J as well as the impact strength (toughness) in kJ/m^2 · (Mansor et al., 2021)

Figure 5: The impact test setup.

3.0 RESULTS AND DISCUSSION

3.1 Density & Porosity

The measured values of Density and porosity were mentioned in Table 6. These values were measured using the equations (1) and (2). Both the hemp and RH samples showed almost same density. However, the density of RH sample is slightly lower than the hemp fibre-based composite. Commercial sample's density and porosity are higher than the other two fibre-based composites.

Table 6 Density & Porosity test results.

Material	Density	Porosity
Hemp fiber-based sample	1.407 g/cm^3	0.713%
RH-based sample	1.40615 g/cm^3	0.8518%
Commercial sample	1.673 g/cm^3	0.937%

3.2 Hardness

The specimens are 25 mm wide and 20 mm long and were created for the Rockwell-B hardness test in accordance with ASTM D785 specifications for composites. The hemp fibre based composite samples' respective hardness values are 84.5, 91.7, 90.8, 84.7, and 90.4 HRR. RH based composite samples' respective hardness values are 95.9, 92.3, 96.5, 89.2 and 91.4 HRR. The average hardness of hemp fibre composite is 88.42 HRR. The average hardness of RH composite is 93.06 HRR. The hardness of commercial brake material is 89.7 HRR. (Budati et al., 2023)

Hemp fibre-based sample showed less hardness than the commercial brake material. The RH-based sample showed a bit higher hardness than the commercial brake material.

3.3 Block-On-Ring

The tribological behaviour of both hemp and RH composites were analysed under dry and wet conditions against steel wheel. Table 7 and Figure 6 shows the wear behaviour. Lowest volume loss and wear rate were observed in RH composite in wet condition. Compared to dry condition wear rate is less in wet condition. This is because of the presence of water medium between the brake block sample and wheel (steel ring). Additionally, the development of secondary structures on the friction surfaces of composites consisting of hemp and RH was taken into consideration while discussing wear-related data. The latter were created from both the corresponding materials waste and oxidised particles. Which is why the steel ring was polished after every use. The same methodology was used in these experiments to analyse micrographs of the friction/wear surfaces of all examined samples and counterparts (Composites et al., 2021). However, in all situations the volume loss is higher than the commercial brake block material. High RH hardness was unable to withstand wear because of the sliding counterpart motion.

Table 7: The wear area, Brugger value, specific wear rate and volume loss at load 12 N under dry and wet conditions for 60 minutes.

Friction condition	**Wear area (mm^2)**	**Brugger value (g/mm^2)**	**Specific wear rate (mm^3/Nm)**	**Volume loss (cm^3)**
Hemp dry	60.247	19.918	0.164×10^{-2}	0.0737
Hemp wet	42.491	27.256	$1.15\times10^{\wedge-3}$	0.05149
RH dry	64.474	18.6121	0.313×10^{-2}	0.099776
RH wet	40.574	29.338	$1.01\times10^{\wedge-3}$	0.045386
Commercial brake block (Budati et al., 2023)	89.824	0.1336 N/mm^2	$2.8786\times10^{\wedge-2}$	0.02104

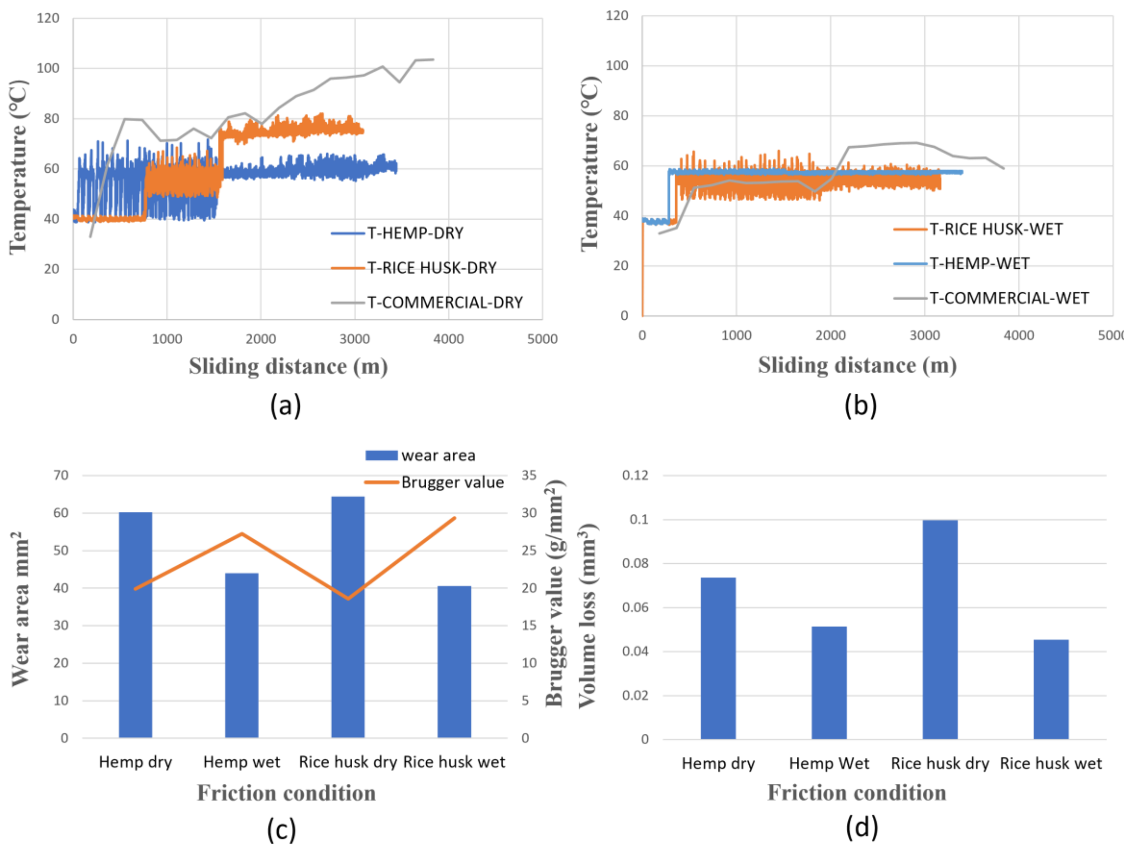

Figure 6: The results for hemp, RH and commercial sample composite at 12 N under dry and wet conditions. (a) The behaviour of temperature with sliding distance in dry conditions, (b) The behaviour of temperature with sliding distance in wet conditions, (c) wear area, Brugger value, (d) Volume loss.

The composites temperatures varied from 38 °C to 81 °C. According to the analytical findings, the combined effect of the heat produced by the two components steel ring and counterpart determines the nominal temperature rise of the shared wear track, whereas the rise in temperature at the shared wear track region depends on its unique properties and operating circumstances. Therefore, the greatest value controls the performance of the system even though distinct temperature maxima can coexist in the shared wear track. (Lin et al., 2023) The Figure 6 shows the temperature behaviour of hemp and RH composites along with sliding distance. Sudden increase of temperature in stages is observed in dry condition. This may be because larger fibre content causes particle agglomeration, which reduces interfacial adhesion. The temperatures increased with increasing sliding distance. It is observed that the temperatures rise in both hemp and RH composites wet conditions is uniform. This is because of the cooling effect from water. High temperature is generated in hemp composite samples than the RH composite.

3.4 Microscopic Images of Worn Surfaces

The hemp and RH composite samples worn out areas surface morphology was studied using Dino-Lite digital microscope. Figure 7 (A) shows the worn surfaces of hemp fibre based composite sample run in dry condition for 60 minutes. The presence of residual fractures occurred at the end of the block. The composite brake block in this instance experienced the most severe failure, as evidenced by fissures that were roughly 5.8 mm wide and 2.1 mm deep. The observations show that the back block, where the face is not in touch with the wheels, has not sustained any substantial damage. However, compared to the rest of the block, the block's edge is similarly cracked and fractured. Figure 7 (C) & (F) shows the commercial samples wear area in dry and wet conditions respectively. Figure 7 (B) shows the RH composite sample run in dry condition for 60 minutes. There are no significant damages on the worn-out area and at edges of the brake block. Fiber-matrix adhesion has a significant impact on the bonding of the interface microstructure, which regulates key mechanical properties of the bio composites. (Prabhu, 2022)To effectively transfer stress and increase the composite's mechanical properties, there must be good interfacial bonding between the fibre and matrix. (Maleque et al., 2012) Figure 7 (D) & (E) shows the worn-out surfaces of hemp and RH composite samples in wet condition. The wear is slightly less than the dry condition. This is due to the aqueous medium that is present between the brake block and wheel. This also contributes to lowering the temperature that friction between the brake block and the wheel generates. This explains why there aren't any noticeable damages in these samples. However, the wear rate in RH composite sample is slightly higher than the wear rate in hemp composite sample in dry condition. But, contradictorily, the wear rate in RH sample is lower than the wear rate in hemp composite in wet condition. This explains that RH fibre has better wear behaviour than hemp fibre in wet condition.

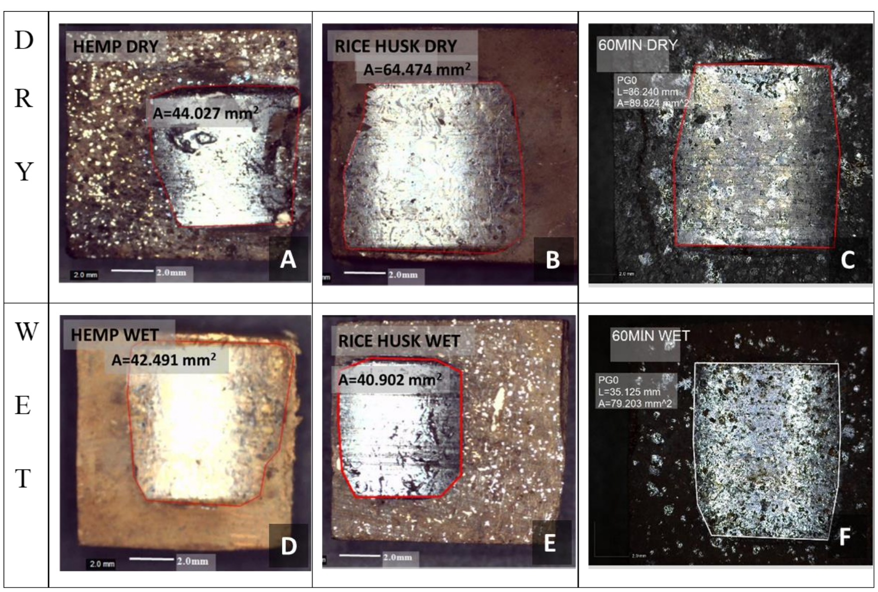

Figure 7: Worn out surfaces of A) Hemp composite in dry condition (HEMP DRY) B) RH composite in dry condition (RICE HUSK DRY) C) Commercial sample dry condition D) Hemp composite in wet condition (HEMP WET) E) RH sample in wet condition (RICE HUSK WET) F) Commercial sample wet condition.

3.5 Impact Test

The impact strength properties of hemp and RH composites are shown in Figure 8. The total energy needed to break the specimen is known as the absorbed impact energy (J) (Srinivasa & Bharath, 2011). The difference between the potential energy before and after the test is used to calculate it. By dividing the observed impact energy that was absorbed by the cross-section area of the samples, the impact strength of the composite (kJ/m^2) was calculated (Ige et al., 2019).

The results clearly showed that the RH composite has showed better impact strength than the hemp composite. The aspect ratio of RH was higher than hemp, thus the shift of stress from the matrix to fibre was more effective.

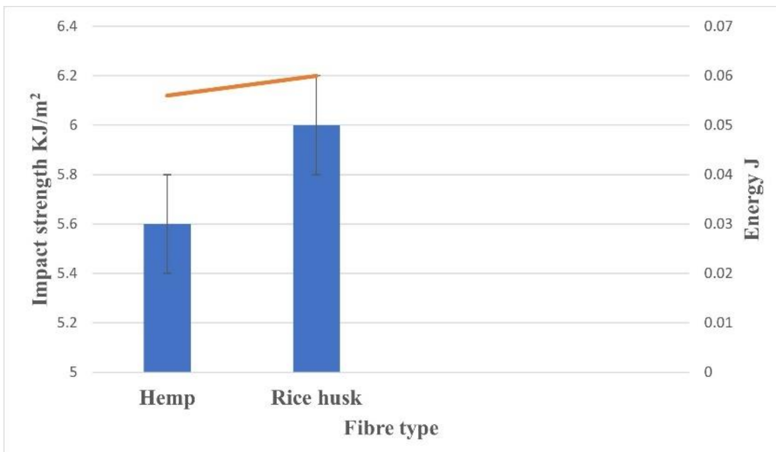

Figure 8: Impact energy and impact strength of hemp and RH composites.

CONCLUSIONS

Dry and wet condition tribology wear tests of hemp and RH composites fabricated by hot compression process were evaluated against 45 HRC steel ring. The results from these tests are summarized as follows:

a) The RH composite showed higher hardness than the hemp composite and commercial sample. However, RH's hardness was unable to withstand wear because of the sliding counterpart motion. The specific wear rate of RH is higher than the hemp.
b) The density of RH sample is slightly lower than the hemp fibre-based composite. even though the density is same as the commercial sample the porosity levels of RH and hemp samples are very low compared to commercial brake block material.
c) Rise of temperature was observed with increase in sliding distance. Maximum temperature of 81 °C was occurred during the wear testing of RH composite in dry sliding condition.
d) Microscopic images showed good interfacial bonding between the fibre, and resin. Severe crack was observed on the hemp composite's sample in dry sliding condition.

From the results it can be concluded that both the RH and hemp composite samples can be used as friction materials.

ACKNOWLEDGMENTS

The authors would like to thank all the staffs and technicians from the Department of Mechanical and Manufacturing Engineering, Faculty of Engineering, University Putra Malaysia, and Tribology Laboratory, Special thanks to Kuasa Rail Engineering Sdn. Bhd. For the commercial rail brake samples. The project is collaborative research between the Department of Mechanical and Manufacturing Engineering, Faculty of Engineering, University Putra Malaysia, and Kuasa Rail Engineering Sdn. Bhd.

REFERENCES

Ademoh, N. A., & Olabisi, A. I. (2015). Development and Evaluation of Maize Husks (Asbestos-Free) Based Brake Pad. Industrial Engineering Letters, 5(2), 67–80.

Anggraeni, S. R. I., Anshar, A. N., Maulana, A., Nurazizah, S., Nurjihan, Z., Putri, S. R., Bayu, A., & Nandiyanto, D. (2022). MECHANICAL PROPERTIES OF SAWDUST AND RICE HUSK BRAKE PADS WITH VARIATION OF COMPOSITION AND PARTICLE SIZE. 17(4), 2390–2401.

Article, R., Bisht, N., Gope, P. C., & Rani, N. (2020). Rice husk as a fibre in composites: A review. 147–162.

Basim Abdul-Hussein, A., Saadi AL-Hassani, E., & Alaa Mohammed, R. (2015). Effect of Nature Materials Powders on Mechanical and Physical Properties of Glass Fiber / Epoxy Composite. Engineering and Technology Journal, 33(1A), 175–197. https://doi.org/10.30684/etj.33.1a.14

Bayu, A., Nandiyanto, D., Fatimah, S., Ragadhita, R., Novia, D. W. I., & Husaeni, A. L. (2022). PARTICLE SIZE AND PORE SIZE OF RICE HUSK ASH ON THE RESIN-BASED BRAKE PADS PERFORMANCE: EXPERIMENTS AND BIBLIOMETRIC LITERATURE REVIEW. 17(6), 4065–4081.

Budati, S., Leman, Z., Sulaiman, M. H., Hanim, M. A., & Ghazali, M. J. (2023). An investigation into the physical, mechanical, tribology, thermal and durability performance of commercial brake material for rail transportation. Proceedings of the Institution of Mechanical Engineers, Part J: Journal of Engineering Tribology. https://doi.org/10.1177/13506501231151719

Composites, H. S. P., Panin, S. V, Luo, J., Buslovich, D. G., Alexenko, V. O., Kornienko, L. A., Bochkareva, S. A., & Byakov, A. V. (2021). Experimental — FEM Study on Effect of Tribological Load Conditions on Wear Resistance of Three-Component.

Idris, U. D., Aigbodion, V. S., Abubakar, I. J., & Nwoye, C. I. (2015). Eco-friendly asbestos free brake-pad: Using banana peels. Journal of King Saud University - Engineering Sciences, 27(2), 185–192. https://doi.org/10.1016/j.jksues.2013.06.006

Ige, O. E., Inambao, F. L., & Adewumi, G. A. (2019). Effects of Fiber, Fillersand Binders on Automobile Brake Pad Performance: a Review. International Journal of Mechanical Engineering and Technology (IJMET), 10(6), 135–150. http://www.iaeme.com/IJMET/index.asp135http://www.iaeme.com/ijmet/issues.asp?JType=IJMET&VType=10&IType=6http://www.iaeme.com/IJMET/issues.asp?JType=IJMET&VType=10&IType=6

Ikpambese, K. K., Gundu, D. T., & Tuleun, L. T. (2016). Evaluation of palm kernel fibers (PKFs) for production of asbestos-free automotive brake pads. Journal of King Saud University - Engineering Sciences, 28(1), 110–118. https://doi.org/10.1016/j.jksues.2014.02.001

Jeganmohan, S., Sugozu, B., Kumar, M., & Selvam, D. R. (2020). Experimental Investigation on the Friction and Wear Characteristics of Palm Seed Powder Reinforced Brake Pad Friction

Composites. Journal of The Institution of Engineers (India): Series D, 101(1), 61–69. https://doi.org/10.1007/s40033-020-00210-9

Le Bell-Rönnlöf, A. M., Lahdenperä, M., Lassila, L., & Vallittu, P. (2007). Bond strength of composite resin luting cements to fiber-reinforced composite root canal post. Journal of Contemporary Dental Practice, 8(6), 17–24. https://doi.org/10.5005/jcdp-8-6-17

Lin, Z., Qu, T., Zhang, K., Zhang, Q., Wang, S., Wang, G., Gao, B., & Fan, G. (2023). Modeling of contact temperatures and their influence on the tribological performance of PEEK and PTFE in a dual-pin-on-disk tribometer. Friction, 11(4), 546–566. https://doi.org/10.1007/s40544-022-0615-8

Maleque, M. A., Atiqah, A., Talib, R. J., & Zahurin, H. (2012). New natural fibre reinforced aluminium composite for automotive brake pad. International Journal of Mechanical and Materials Engineering, 7(2), 166–170.

Mansor, M. R., Mustafa, Z., Hadi, M. A. A., Taufiq, M. J., Masripan, N. A., & Ratanawilai, T. (2021). Effect of layering sequence on mechanical properties of hybrid oil palm empty fruit bunch / kenaf fibre reinforced epoxy composites. 29(February), 1–10.

Naidu, M., Technical, S., Society, E., Bacche, D., Dhage, S., & Bhosale, A. A. (2020). An Insight on the Influence of Fiber Content on Plant Fiber Reinforced Brake an Insight on the Influence of Fiber Content on Plant Fiber Reinforced Brake. January 2021.

Palanivel, M. (2019). Development and Study of Tribological Properties of Biocomposite for Brake Pad Application DEVELOPMENT AND STUDY OF TRIBOLOGICAL PROPERTIES OF. June. https://doi.org/10.24247/ijmperddec201729

Patel, M., Sahu, S. K., Singh, M. K., & Sahu, D. P. (2022). Investigation of tribological properties of stir cast AA5052 / B 4 C MMC under different loads. 34(August 2021), 69–86.

Prabhu, S. (2022). An experimental investigation on tribological characteristics of graphite / MWCNT mixed hybrid cutting fluids. 35(August 2021), 16–32.

Rao, R. U., & Babji, G. (2015). A Review paper on alternate materials for Asbestos brake pads and its characterization. 556–562.

Rashid, B., Leman, Z., Jawaid, M., Ghazali, M. J., & Ishak, M. R. (2016). Physicochemical and thermal properties of lignocellulosic fiber from sugar palm fibers: effect of treatment. Cellulose, 23(5), 2905–2916. https://doi.org/10.1007/s10570-016-1005-z

Shahril, S. M., Ridzuan, M. J. M., Majid, M. S. A., Bariah, A. M. N., Rahman, M. T. A., & Narayanasamy, P. (2022). Alkali treatment influence on cellulosic fiber from Furcraea foetida leaves as potential reinforcement of polymeric composites. Journal of Materials Research and Technology, 19, 2567–2583. https://doi.org/10.1016/j.jmrt.2022.06.002

Singh, T., Patnaik, A., Chauhan, R., & Rishiraj, A. (2017). Assessment of braking performance of lapinus–wollastonite fibre reinforced friction composite materials. Journal of King Saud University - Engineering Sciences, 29(2), 183–190. https://doi.org/10.1016/j.jksues.2015.06.002

Srinivasa, C. V., & Bharath, K. N. (2011). Impact and hardness properties of areca fiber-epoxy reinforced composites. Journal of Materials and Environmental Science, 2(4), 351–356.

V, P. K., Nivetha, S. K., S, B. P., Raman, K., & S, S. K. V. (2021). Characterization and analysis of AA1100 - SiC p metal matrix composite fabricated through friction stir processing. 29(February), 31–40.